Journal of Macromolecular Science, Part A
Publication details, including instructions for authors and subscription information:
http://www.informaworld.com/smpp/title~content=t713597274

Synthesis of Poly(Methyl Methacrylate)/Silica Nano-composites. III. Block Copolymer with Lamellar Structure

Yasutaka Mori[a]; Reiko Saito[a]
[a] Department of Organic and Polymeric Materials, Tokyo Institute of Technology, Ookayama, Meguro, Tokyo, Japan

Online publication date: 05 December 2003

To cite this Article Mori, Yasutaka and Saito, Reiko(2003) 'Synthesis of Poly(Methyl Methacrylate)/Silica Nano-composites. III. Block Copolymer with Lamellar Structure', Journal of Macromolecular Science, Part A, 40: 7, 671 — 688
To link to this Article: DOI: 10.1081/MA-120021418
URL: http://dx.doi.org/10.1081/MA-120021418

MARCEL DEKKER, INC. • 270 MADISON AVENUE • NEW YORK, NY 10016

JOURNAL OF MACROMOLECULAR SCIENCE®
Part A—Pure and Applied Chemistry
Vol. A40, No. 7, pp. 671–688, 2003

Synthesis of Poly(Methyl Methacrylate)/Silica Nano-composites. III. Block Copolymer with Lamellar Structure

Yasutaka Mori* and Reiko Saito

Department of Organic and Polymeric Materials, Tokyo Institute of Technology, Ookayama, Meguro, Tokyo, Japan

ABSTRACT

Three types of poly(methyl methacrylate)-*block*-poly(methyl methacrylate-*co*-2-hydroxyethyl methacrylate) [PMMA-*block*-P(MMA-*co*-HEMA)] block-random copolymer and two types of poly(methyl methacrylate)-*block*-poly(2-hydroxyethyl methacrylate) [PMMA-*block*-PHEMA] were synthesized by atom transfer radical polymerization as precursor polymers for PMMA/silica nano-composites. Nano-composite films of PMMA/silica were synthesized by the reaction of perhydropolysilazane (PHPS) with precursor polymers in 1,4-dioxane and the cast of the 1,4-dioxnae solutions. The effects of the localization of HEMA unit in PMMA-*block*-P(MMA-*co*-HEMA) block-random copolymer and the amount of PHPS to HEMA in feed on the microphase separation of nano-composites were investigated. Microphase separation of the nano-composites was observed by transmission electron microscopy (TEM) and scanning electron microscopy (SEM). It was found that the sub-micrometer silica domains were homogeneously dispersed in a wide area in the nano-composites. The thermal properties of the nano-composites were measured by differential scanning calorimetry and thermogravimetric analysis.

Key Words: PMMA; Silica; Perhydropolysilazane; Block copolymer; Nano-composite.

*Correspondence: Yasutaka Mori, Department of Organic and Polymeric Materials, Tokyo Institute of Technology, 2-12, Ookayama, Meguro, Tokyo 152-8552, Japan; Fax: +81-3-5734-2937; E-mail: ymori@polymer.titech.ac.jp.

DOI: 10.1081/MA-120021418 1060-1325 (Print); 1520-5738 (Online)

INTRODUCTION

Many studies on polymer/silica nano-composites have been carried out because of their high functionalities such as high transparency, high mechanical strength, high thermal stability, etc.[1–5] Recently, sol–gel method is the most popular method for synthesis of the polymer/silica nano-composites. The sol–gel method can be carried out at lower than 200°C and be applied to many polymers.[6–12] However, the sol–gel method has disadvantages. Silica synthesized by the sol–gel method at lower than 200°C contains many lattice defects. As a result, the properties of silica synthesized by the sol–gel method are different from those of quartz glass. To obtain silica glass, which properties are close to those of quartz glass, the silica should be annealed over 500°C. It is impossible to obtain polymer/silica composites without lattice defects by the sol–gel method.

On the other hand, perhydropolysilazane (PHPS) is converted to silica without lattice defect by calcination at lower than 100°C under steam.[13,14] The properties of silica made from PHPS are close to those of amorphous quartz glass.

PHPS is highly reactive with hydroxyl groups. In previous work, PMMA/silica-rich nano-composites were obtained by the reaction of PHPS with hydroxyl groups of poly(methyl methacrylate-*co*-2-hydroxyethyl methacrylate) [P(MMA-*co*-HEMA)].[15] The PMMA/silica-rich nano-composite with lamellar of PMMA and silica-rich domains was obtained when the molar fraction of HEMA in P(MMA-*co*-HEMA) and the molar ratio of PHPS to HEMA were 0.145 and 1.5, respectively. The average domain spacing of lamellar was 110 nm. However, other morphologies such as sphere and cylinder were not observed for PMMA/silica-rich composites synthesized with the random copolymers.

Block copolymer with incompatible sequences forms microphase separation. Based on Molau's law, the morphology of the microphase separation is governed by the volume fraction of each block of block copolymer.[16] The control of the morphology of microphase separation of PMMA/silica-rich nano-composites was expected with block copolymers with PHPS sequence by varying the volume fraction of the PHPS sequence.

Based on this consideration, the PMMA/silica-rich nano-composites was synthesized by blending poly(methyl methacrylate)-*block*-poly(2-hydroxyethyl methacrylate) (PMMA-*block*-PHEMA) and PHPS.[17] To obtain silica-rich spheres, PMMA-*block*-PHEMA with volume fraction of PMMA, 0.74, was used. The morphology of PMMA/silica-rich composites synthesized with block copolymer of PHEMA-sphere was not strictly controlled by varying amount of PHPS in feed. The PHPS content in the block copolymer was not changed widely because the volume fraction of P(MMA-*co*-HEMA) was low. Additionally, it was found that the distance between hydroxyl groups should be larger than the diameter of PHPS molecule. To increase the PHPS amount introduced in the block copolymer by increasing the distance between hydroxyl groups, PMMA-*block*-P(MMA-*co*-HEMA) block-random copolymers instead of PMMA-*block*-PHEMA were used. PMMA-*block*-P(MMA-*co*-HEMA) block-random copolymer consisted with PMMA homopolymer sequence and the sequence of random copolymer of P(MMA-*co*-HEMA). The molar amount of PHPS introduced to HEMA in block copolymer was improved up to 0.3 for PMMA-*block*-P(MMA-*co*-HEMA) block-random copolymers. However, the morphology was not strictly controlled.

The aim of this work is to control the morphology of composites by changing the volume fraction of the sequence of PMMA-*block*-P(MMA-*co*-HEMA) block-random copolymers. To obtain the microphase separated films with the morphologies of PMMA spheres and lamellae of PMMA/silica-rich domains, PMMA-*block*-P(MMA-*co*-HEMA) block-random copolymers with volume fractions of PMMA block sequence, 0.52–0.56 and 0.21, respectively, were synthesized. Increasing of the volume fractions of P(MMA-*co*-HEMA) sequence in the block-random copolymers will lead to the wide change of the morphology of microphase separation. To change the average distance between hydroxyl groups, the molar fraction of PHEMA unit in P(MMA-*co*-HEMA) sequence was varied. The morphology of the microphase separation was investigated by transmission electron microscopy and scanning electron microscopy. Thermal properties of nano-composites were measured by thermogravimetric analysis and differential scanning calorimetry.

EXPERIMENTAL

Materials

Methyl methacrylate (MMA) and 2-hydroxyethyl methacrylate (HEMA) were purified by distillation under vacuum. 1,4-Dioxane (DIOX) and n-hexane were dried with sodium metal and distilled under vacuum. Benzene, methanol, 2-butanone, 1-propanol, dimethlysulfoxide (DMSO), tetrahydrofurane (THF), phenyl isocyanate (Kanto Chemicals Co., Ltd.), methyl 2-chloropropionate (MCP, Tokyo Kasei Kogyo Co., Ltd.), copper (I) chloride (CuCl, Wako Pure Chemical Industries, Ltd.), 1,1,4,7,10,10-hexamethyltriethrenetetramine (HMTETA, Aldrich), and perhydropolysilazane (PHPS)/xylene solution (NN-110, Clariant Japan Co., PHPS = 20 wt%, M_n = 700) were used as received. Several types of poly(methyl methacrylate-*block*-2-hydroxyethyl methacrylate)(PMMA-*block*-PHEMA) and PMMA-*block*-P(MMA-*co*-HEMA) block-random copolymers were synthesized by the method previously reported.[16] The conditions and results of ATRP for PMMA macroinitiators were listed in Table 1. Those for PMMA-*block*-PHEMA and PMMA-*block*-P(MMA-*co*-HEMA) block-random copolymers were listed in Table 2.

Table 1. Conditions and results of ATRP of PMMA macroinitiator.

Code	MCP[a] (mM)	MMA (M)	CuCl (mM)	Ligand (mM)	M_n[b] (kg/mol)	M_w/M_n[c]
A	41.7	4.75	41.5	41.4	28.8	1.31
B	105.3	4.75	49.3	49.6	21.4	1.20
C	52.6	4.75	50.1	51.5	24.9	1.26
D	131.6	4.75	96.8	95.6	15.9	1.16

Solvent: MEK/1-PrOH (7/3 v/v), reaction time: 180 min, temperature: 50°C.
[a] Methyl 2-chloropropionate.
[b] Number average molecular weight determined by GPC.
[c] Polydispersity determined by GPC.

Table 2. Conditions and results of ATRP for $PMMA_1$-*block*-P(MMA_2-*co*-HEMA).

Code	PMMA macroinitiator	[Initiator]:[MMA]:[HEMA]	Reaction time (min)	M_n[a] (kg/mol)	M_w/M_n[b]	Volume fraction (vol%) [upper] and molar fraction (mol%) [lower][c]			Distance between hydroxyl groups (nm)
						MMA_1	MMA_2	HEMA	
L25	A	1.00:913:264	120	50.0	1.26	0.564	0.315	0.121	2.22
						0.576	0.321	0.103	
L50	B	1.00:478:414	70	39.5	1.31	0.518	0.217	0.265	1.10
						0.542	0.227	0.231	
R50	D	1.00:737:638	420	76.8	1.25	0.194	0.438	0.368	1.33
						0.207	0.466	0.327	
L100	A	1.00:0:1093	60	56.8	1.56	0.462	0	0.538	0.57
						0.507	0	0.493	
R100	C	1.00:0:2040	175	105	1.33	0.207	0	0.793	0.57
						0.238	0	0.762	

Solvent: MEK/1-PrOH (7/3 v/v), temperature: 50°C, [Initiator] : [CuCl] : [Ligand] = 1:1:1.

[a] Determined by GPC by calibration with linear PMMA standards for L25, L50 and R50. Determined by combining GPC and ^{1}H-NMR for L100 and R100.

[b] Determined by GPC.

[c] MMA_1, MMA_2, and HEMA indicate the sequences of $PMMA_1$-*block*-P(MMA_2-*co*-HEMA), respectively. Molar fraction was determined by ^{1}H-NMR.

MARCEL DEKKER, INC. • 270 MADISON AVENUE • NEW YORK, NY 10016

Characterization of PMMA-*block*-PHEMA and PMMA-*block*-P(MMA-*co*-HEMA)

Number-average molecular weight (M_n) and polydispersity index (M_w/M_n) of polymer was measured with a gel permeation chromatograph (GPC, TOSOH HPLC-8020) with TSKgelG5000H_{HR} column and THF at 35°C. For GPC measurements, the hydroxyl group of polymer was modified with phenyl isocyanate. M_n and M_w/M_n of polymer were calculated with calibration curves of PMMA.

The Content of HEMA in polymer was measured with ^{1}H-NMR (JEOL, GLX-500, 500 MHz). Deuterized DMSO was used as a solvent. The peak at 3.6 ppm (hydrogen in methyl ester of MMA and in methylene next to carbonyl group of HEMA) and 3.8 ppm (hydrogen in methylene next to hydroxyl group of HEMA) were used to measure the content of HEMA unit in polymer.

PMMA/Silica-Rich Composites

PMMA/PHPS-rich composites were prepared by reaction of hydroxyl group of HEMA and PHPS. Polymer/DIOX (polymer concentration: 1 w/v%) solution and NN-110 were mixed under nitrogen atmosphere. The solution was stored for reaction at room temperature for 24 h. In order to investigate the introduced amount of PHPS in the polymer, a small amount of the solution was sampled and precipitated with n-hexane for removing of un-reacted PHPS. The content of PHPS in the polymer was measured with a Fourier-transfer infrared spectrometer (JASCO, FT/IR-410). The absorption at 1730 cm^{-1} (carbonyl group in methacrylates) and 2250 cm^{-1} (Si—H bonding in PHPS) were used. After the reaction, the solution was cast on a Teflon dish under nitrogen atmosphere. For calcination, PMMA/PHPS-rich films were exposed with a 5 vol% triethylamine aqueous solution as catalyst for 2 min, then calcinated at 90°C for 2 h under steam.

Transmission Electron Microscopy (TEM)

A drop of polymer/PHPS solution was cast on a copper microgrid coated with carbon substrate and dried for 2 days at room temperature. The calcination of specimen was carried out as well as described above. Microphase separation of film was observed with a transmission electron microscope (JEOL, JEM-200CX) at 120 kV without staining.

Scanning Electron Microscopy (SEM)

The surface of PMMA/silica-rich composite films was smoothed with a microtome (Leica, ULTRACUT-UCT) with glass knives. In order to remove organic compound in the composites, the surface was exposed to fire for a few second. The specimen was spattered with Pt-Pd with an ion-spatter (Hitachi, E-1030) at 15 mA. Observed images were recorded with a scanning electron microscope (Hitachi, S-800) at 15 kV.

MARCEL DEKKER, INC. • 270 MADISON AVENUE • NEW YORK, NY 10016

Differential Scanning Calorimetry (DSC)

5 mg of specimen was sealed in an aluminum pan and measured with a differential scanning calorimeter (Seiko Instruments Inc., DSC-220C) under nitrogen atmosphere. The measurement was performed from 50 to 200°C at a heating rate of 20°C/min.

Thermogravimetric Analysis (TGA)

5 mg of specimen was sealed into an Al pan and measured with a thermogravimetric analyzer (Seiko Instruments Inc., EXSTAR6000TG/DTA6300) under nitrogen atmosphere. The measurement was conducted from 50 to 600°C at a heating rate of 10°C/min.

RESULTS AND DISCUSSION

Synthesis of PMMA-*block*-P(MMA-*co*-HEMA) Block-Random Copolymers

In the previous study, the introduced amount of PHPS into the PMMA-*block*-PHEMA block copolymer was less than that into the PMMA-*block*-P(MMA-*co*-HEMA) block-random copolymer because the distance between hydroxyl groups in PHEMA sequence of PMMA-*block*-PHEMA was less than the diameter of a PHPS molecule.[17] To obtain well-ordered morphology, the polydispersity of the molecular weight (M_w/M_n) of the block-random copolymers should be decreased. Atom transfer radical polymerization (ATRP) is a useful synthetic method for polymethacrylates with controlled molecular weight and narrow distribution of molecular weight.[18–21] The conditions and results of ATRP for PMMA macroinitiators were listed in Table 1. The M_w/M_n of the PMMA macroinitiators were less than 1.31. Taking account of low M_w/M_n of PMMA macroinitiators, these were used for synthesis of PMMA-*block*-PHEMA and PMMA-*block*-P(MMA-*co*-HEMA) block-random copolymers. The conditions and results of ATRP for PMMA-*block*-PHEMA and PMMA-*block*-P(MMA-*co*-HEMA) block-random copolymers were listed in Table 2. To vary the distance between hydroxyl groups, not only PMMA-*block*-PHEMA but also PMMA-*block*-P(MMA-*co*-HEMA) block-random copolymers were synthesized by ATRP. For the morphologies of microphase separation of PMMA lamellar and PMMA spherical domains, the preferable volume fractions of PMMA are in ranges from 0.4 to 0.6 and from 0.15 to 0.25, respectively. The volume fractions of PMMA block sequence were 0.518–0.564 and 0.207 for L-series and R-series, respectively The morphologies of microphase separation of PMMA lamellar and PMMA spherical domains were expected for L-series and R-series, respectively. The M_w/M_n of the block copolymers were less than 1.56. The morphology of the microphase separation was expected to be homogeneous. The volume fraction of PMMA in PMMA-*block*-P(MMA-*co*-HEMA) block-random copolymers was determined by the molecular weights and densities of each sequence. The density of P(MMA-*co*-HEMA) sequence was calculated by an average value of the densities of PMMA and PHEMA. The densities of PMMA and PHEMA at 25°C used for calculation are 1.188 g/cm^3,[22] and 1.289 g/cm^3,[23] respectively. The molar fraction of HEMA unit in

P(MMA-*co*-HEMA) block were varied in the range between 0.243 and 0.504. The ratios of the distances between hydroxyl groups in P(MMA-*co*-HEMA) sequence of PMMA-*block*-P(MMA-*co*-HEMA) block-random copolymers to an average diameter of PHPS molecules in NN-110, 0.89 nm were in a range from 1.24 to 2.49. Since the values of monomer reactivity ratio of random copolymerization at 60°C, r_1 and r_2, where monomer 1 is MMA and monomer 2 is HEMA, are 0.824 and 0.63, respectively,[24] the gradient of composition of HEMA in the P(MMA-*co*-HEMA) block sequence was neglected.

Reaction of PHPS and PMMA-*block*-P(MMA-*co*-HEMA) Block-Random Copolymers

PMMA-*block*-PHEMA block copolymers, L100 and R100, were not dissolved in DIOX. Thus, PMMA-*block*-P(MMA-*co*-HEMA) block-random copolymers were used for the synthesis of PMMA/silica-rich composite in DIOX. Conditions and results of the synthesis of the composites were listed in Table 3. In this study, gelation of the systems was not observed for all PMMA-*block*-P(MMA-*co*-HEMA) block-random copolymers.

The conversion of PHPS with PMMA-*block*-P(MMA-*co*-HEMA) block-random copolymers was estimated by FT-IR. To purify the polymer, polymer was precipitated with an excess amount of n-hexane, which is a good solvent for PHPS. Figures 1(a and b) show FT-IR spectra of L50 and the composite with L50 at $\phi_f = 1.0$ after purification, where ϕ_f is the molar ratio of PHPS to hydroxyl groups in feed. After the reaction, new

Table 3. Conditions and results of the synthesis of the nano-composites.

					Volume fractions[d]		
						Silica-rich	
Code	Polymer	ϕ_f[a]	ϕ_p[b]	Conversion (mol%)[c]	$PMMA_1$	Silica (reacted)	Silica (un-reacted)
L25-0.5	L25	0.5	0.087	17.4	0.450	0.383	0.167
L25-1.0	L25	1.0	0.185	18.5	0.374	0.351	0.275
L25-1.5	L25	1.5	0.265	17.6	0.320	0.323	0.356
L50-0.5	L50	0.5	0.150	29.9	0.333	0.416	0.251
L50-1.0	L50	1.0	0.192	19.2	0.245	0.329	0.426
L50-1.5	L50	1.5	0.228	15.2	0.194	0.276	0.530
R50-0.5	R50	0.5	0.162	32.4	0.110	0.595	0.295
R50-1.0	R50	1.0	0.184	18.4	0.076	0.428	0.496
R50-1.5	R50	1.5	0.283	18.9	0.059	0.375	0.567

[a] The molar ratio of PHPS to hydroxyl groups in feed.
[b] The molar ratio of introduced PHPS to hydroxyl groups in the polymer.
[c] The conversion of the PHPS reacted with the hydroxyl groups of the polymer.
[d] Volume fraction in the nano-composites. Silica (Reacted): the total volume fraction of $PMMA_2$, PHEMA and silica formed with PHPS reacted with PHEMA. Silica (un-reacted): the volume fraction of silica formed with un-reacted PHPS.

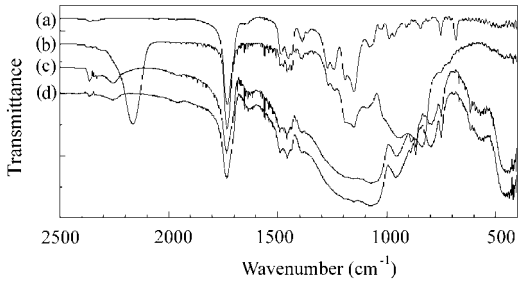

Figure 1. FT-IR spectra of L50 and the composite with L50 at $\phi_f = 1.0$. (a) L50, (b) the purified product of the composite, (c) the composite after casting, (d) the composite after calcination.

peaks appeared at 2250 cm^{-1} and 830 cm^{-1} due to the bonds of Si–H, and Si—N of PHPS, respectively. It was found that PHPS was introduced to PMMA-*block*-P(MMA-*co*-HEMA) block-random copolymers.

The conversion of the reacted PHPS with PMMA-*block*-P(MMA-*co*-HEMA) block-random copolymers was determined by using the peaks at 1730 and 2250 cm^{-1} due to C = O bond of the block-random copolymers and Si—H bond of PHPS, respectively, and shown in Fig. 2 as the molar ratio of introduced PHPS to hydroxyl groups in the polymer (ϕ_p) against ϕ_f. It was previously found that the introduced amounts of PHPS to PMMA-*block*-P(MMA-*co*-HEMA) block-random copolymers with molar fractions of PMMA block sequence and HEMA units in P(MMA-*co*-HEMA) block sequence, 0.81–0.84 and 0.239–0.487, respectively, were saturated at 3 h.[17] In this work, the reaction was carried out for 24 h. Thus, ϕ_p were saturated values. The ϕ_p of the composites are listed in Table 3. For all polymers, ϕ_p was increased with ϕ_f up to 0.25 at $\phi_f = 1.5$. The similar increasing tendency of ϕ_p was previously observed.[15,17]

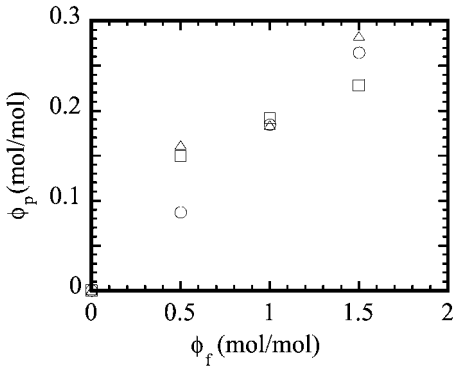

Figure 2. Concentration effect of PHPS in feed on introduction to block copolymers. (○): L25, (□): L50, (△): R50.

MARCEL DEKKER, INC. • 270 MADISON AVENUE • NEW YORK, NY 10016

Synthesis of PMMA/Silica-Rich Composites

PMMA/silica-rich composite films were synthesized by blending PMMA-*block*-P(MMA-*co*-HEMA) block-random copolymers and PHPS without purification. Fig. 1(c) shows the FT-IR spectra of the composite with L50 at $\phi_f = 1.0$ after casting without purification. By casting, the peaks of Si—H bond (2250 cm^{-1}) and Si—N bond (830 cm^{-1}) were drastically decreased. On the other hand, the peaks due to Si—O bond (1100 and 450 cm^{-1}) newly appeared. This indicates that the calcination of PHPS to silica occurred during casting. Figure 1(d) shows the FT-IR spectra of the composite film with L50 at $\phi_f = 1.0$ without purification after calcination at 90°C. The FT-IR spectra before and after calcination showed a good agreement. The calcination of PHPS to silica of the composites was completed without heating. It should be noticed that all composite films were transparent, except for the composites with R50 at $\phi_f = 1.0$ and 1.5.

Morphologies of PMMA/Silica-Rich Composites

The structure of the microphase separation of the composites was investigated by transmission electron microscopy (TEM) and scanning electron microscopy (SEM). The microphase separation was not observed for PMMA-*block*-P(MMA-*co*-HEMA) block-random copolymers because of low segregation of HEMA units in the P(MMA-*co*-HEMA) sequence. In order to compare the morphologies of composites with those of precursor block copolymers, the microphase separation of L100 and R100, PMMA-*block*-PHEMA block copolymers with similar M_n to PMMA-*block*-P(MMA-*co*-HEMA) block-random copolymers, was observed by TEM as references of the PMMA-*block*-P(MMA-*co*-HEMA) block-random copolymers. The TEM micrographs of L100 and R100 stained with OsO_4 are shown in Fig. 3. The dark regions correspond to selectively stained HEMA domains. The volume fractions of PHEMA sequence were 0.538 and 0.793, respectively (Table 2). The morphology of microphase separation of L100 was lamella with 19.2 and 22.3 nm of thickness of PMMA and PHEMA domains, respectively. The morphology of R100 was PMMA spheres with 29.1 nm of an average diameter in a PHEMA matrix. It was found that the microphase separation of L100 and R100 was governed by Molau's law.[16]

Figure 4 shows the TEM micrographs of the composites with L25 and L50. It is possible to observe the silica-rich domains as dark by TEM without staining.

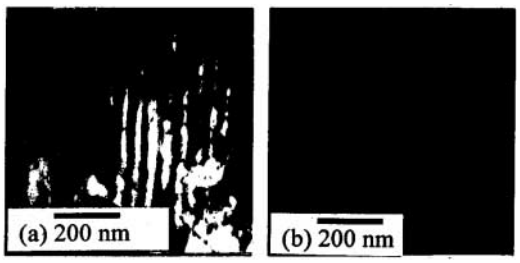

Figure 3. TEM micrographs of PMMA-*block*-PHEMA stained with OsO_4. (a) L100, (b) R100.

MARCEL DEKKER, INC. • 270 MADISON AVENUE • NEW YORK, NY 10016

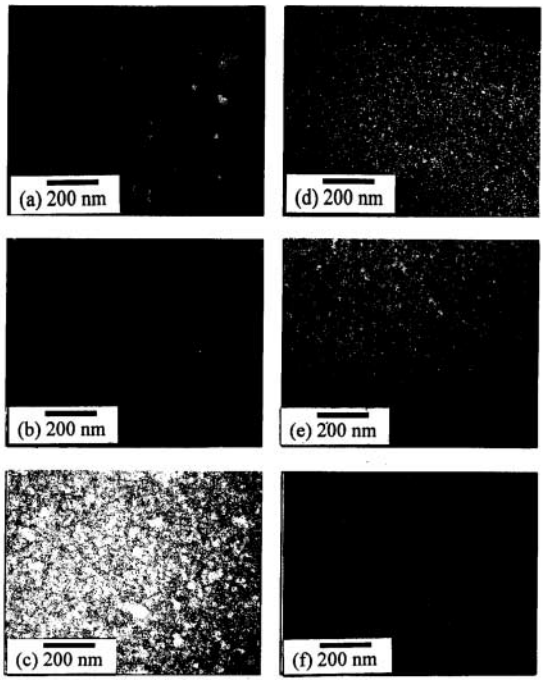

Figure 4. TEM micrographs of the films of the composites with L25 and L50. (a) L50 at $\phi_f = 1.0$, (b) L50 at $\phi_f = 0.5$, (c) L50 at $\phi_f = 1.5$, (d) L25 at $\phi_f = 1.0$, (e) L25 at $\phi_f = 0.5$, (f) L25 at $\phi_f = 1.5$.

The composites were not stained. For all composites, the microphase separation of PMMA and silica-rich domains was observed. Thus, the composites synthesized in this work were PMMA/silica-rich nano-composites. The volume fraction of un-reacted PHPS, which did not react with hydroxyl groups of PHEMA units, was determined with $v_{sil}(1 - \phi_p/\phi_f)$, where v_{sil} is the volume fraction of silica in the nano-composites. The v_{sil} was determined with the amount of PHPS in feed and the density of silica (2.2 g/cm^3,[25]) and PMMA-*block*-P(MMA-*co*-HEMA) block-random copolymers. Taking account of the calcination of PHPS, $[-(SiH_2NH)_n- + 2n\ H_2O \rightarrow n\ SiO_2 + NH_3 + 2\ H_2]$, the ratio of molar densities of silica to PHPS was 1.33. The volume fractions of the domains are listed in Table 3. The morphology of microphase separation of the composite of L50-series at $\phi_f = 1.0$ was spheres of the organic polymers with 25.2 nm of an average diameter in a silica matrix (Fig. 4a). The volume fraction of $PMMA_1$ in the composite with L50 at $\phi_f = 1.0$ was 0.245. Taking account of Molau's law[16] and the value of the volume fraction of $PMMA_1$ in the composite with L50 at $\phi_f = 1.0$, 0.245, it is reasonable that the morphology with the spheres of the organic polymer was observed for the composite with L50 at $\phi_f = 1.0$. Consequently, it was found that the dark domain of the composite with L50 at $\phi_f = 1.0$ was composed of silica and P(MMA-*co*-HEMA) sequence. The distance between the centers of spherical domains of organic polymer of the composite with L50 at $\phi_f = 1.0$ was 66.2 nm.

For the composites with L50 at $\phi_f = 0.5$ (Fig. 4b) and 1.5 (Fig. 4c), the organic domains with 25.0 and 22.1 nm of average diameters, respectively, were observed in the dark silica-rich matrices. The average diameters of the composites with L50 at $\phi_f = 0.5$ and 1.5 were close to the lamellar thickness of the PMMA domain of L100, 19.2 nm, which can be assumed as a reference of L50. The small spherical silica-rich domains (average diameter < 10 nm) were also observed in the composites with L50 at $\phi_f = 0.5$ and 1.5. For the composites with L50, the volume fractions of silica formed with un-reacted PHPS were 0.251 and 0.530 for $\phi_f = 0.5$ and 1.5, respectively. The silica formed with un-reacted PHPS may cause macroscopic separation of the silica-rich domains in the composites, which sizes will be larger than 1 μm. However, the macroscopic domain of silica was not observed in this work. When incompatible homopolymers are blended, the addition of block or graft copolymers, where sequences are compatible to the homopolymers, prevents the macrophase separation. It is because that the block and graft copolymers act as surfactants. When PHPS was grafted onto a PMMA-*block*-P(MMA-*co*-HEMA) block-random copolymer by reaction, the polymer grafted with PHPS would act as the surfactant. Consequently, the silica originated from un-reacted PHPS would form the silica microscopic domains of the composites with L50. For the composites with L50 at $\phi_f = 0.5$ and 1.5, the morphology did not depend on the ϕ_f values.

In the composites with L25 (Fig. 4d–f), small spherical silica-rich domains (average diameter < 10 nm) were homogeneously dispersed. The sizes of the silica-rich domain of the composites with L25 were smaller than the lamellar thickness of the PHEMA domain of L100, 22.3 nm. For the composites with L25, the volume fractions of silica formed with un-reacted PHPS were 0.167, 0.275 and 0.356 for $\phi_f = 0.5$, 1.0 and 1.5, respectively. However, the macroscopic domain of silica was not observed as well as the composite with L50. For the composites with L25, the morphology did not depend on the ϕ_f values. The volume fraction of $PMMA_1$ of the nano-composites with L25 at $\phi_f = 1.0$, 0.320, was close to that of the composite with L50 at $\phi_f = 0.5$, 0.333. However, the microdomains of PMMA with ca. 20 nm were not observed in the nano-composites with L25 at $\phi_f = 1.0$. It was found that not the volume fraction of $PMMA_1$ and silica-rich domains but the HEMA content of the P(MMA-*co*-HEMA) block sequence in the PMMA-*block*-P(MMA-*co*-HEMA) block-random copolymers effected mainly on the morphology of the nano-composites with the L-series polymers.

Figure 5 shows TEM micrographs of the composites with R50. Since the volume fraction of $PMMA_1$ of R50 was 0.207, the spherical PMMA domains in silica-rich matrices were expected for the composites. As expected, for the composites with R50, the spherical domains of organic polymer with average diameters of 28.8, 28.8 and 27.3 nm were observed for $\phi_f = 0.5$, 1.0 and 1.5, respectively. The diameters of the composites with R50 were close to the diameter of PMMA domain of R100, which can be assumed as a reference of R50, 29.1 nm. Since the macrophase separation was not observed for the composites with R50, silica formed with un-reacted PHPS would be included in the silica-rich matrix. The silica-rich domains with a range from 100 to 300 nm were not observed for the composite with R50 at $\phi_f = 0.5$ but for those at $\phi_f = 1.0$ and 1.5. For the composites with R50, it was possible to control the size of silica-rich domain by varying the amount of PHPS in feed. Consequently, for control of the morphology of the nano-composites, it was important to change the composition of precursor polymer rather than the amount of PHPS in feed.

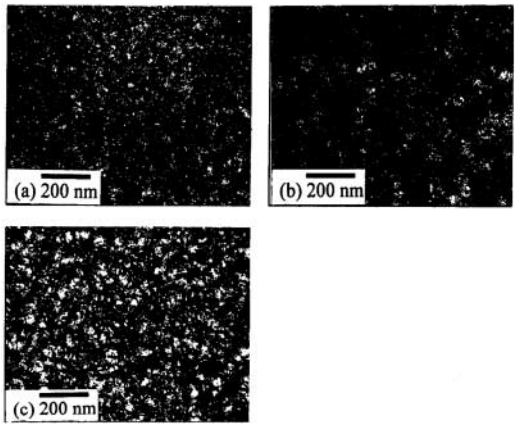

Figure 5. TEM micrographs of films of the composites with R50. (a) $\phi_f = 0.5$, (b) $\phi_f = 1.0$, (c) $\phi_f = 1.5$.

In order to investigate the morphology of PMMA/silica-rich nano-composite films in a wide area, the SEM images of the cross-section of the nano-composites were observed. The SEM micrographs of the composites with L50 and R50 at $\phi_f = 1.0$ are shown in Figs. 6 and 7, respectively. By etching the domains of the organic polymer on the smooth surface of the composite films, the silica-rich domains were observed white. In each SEM micrograph, the sub-micrometer structure of silica-rich domains was observed. The sub-micrometer silica-rich domains were homogeneously dispersed in the wide area of the composite films. The average diameters of silica-rich domains of the composites with L50 and R50 at $\phi_f = 1.0$ were 137 and 295 nm, respectively. As described above, the observed diameters of the silica-rich domains were larger than the expected values. The size of silica-rich domain observed by SEM was agreed to the diameter of the silica-rich domain observed by TEM. As a result, the homogeneous morphology of the microphase separation in the wide area was formed in the nano-composites with the block-random copolymer and PHPS.

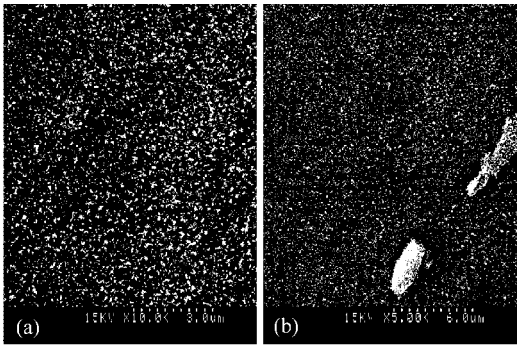

Figure 6. SEM micrographs of cross section of the composites with L50 at $\phi_f = 1.0$. (a) magnification $= 10,000$, (b) magnification $= 5,000$.

MARCEL DEKKER, INC. • 270 MADISON AVENUE • NEW YORK, NY 10016

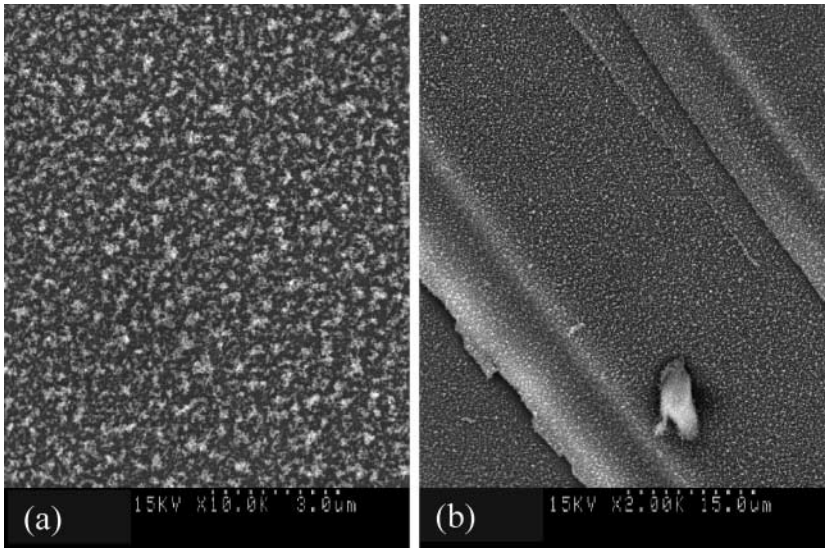

Figure 7. SEM micrographs of cross section of the composites with R50 at $\phi_f = 1.0$. (a) magnification = 10,000, (b) magnification = 2,000.

Thermal Properties of PMMA/Silica-Rich Nano-composites

In order to investigate the hybridization effects of silica on thermal properties of organic polymer, DSC measurement was carried out. Figure 8 shows the DSC curves of L50 and the composites with L50 at $\phi_f = 1.0$ as a typical case. Glass transition temperature (T_g)

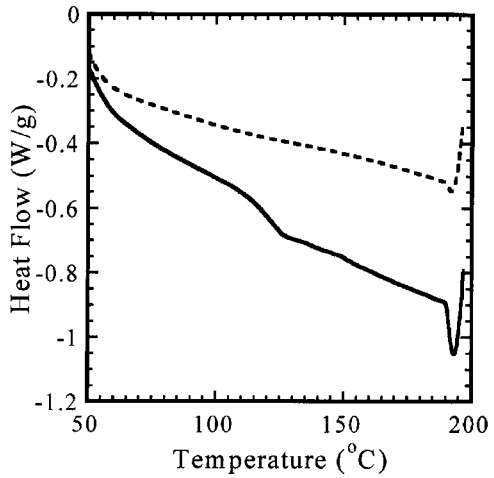

Figure 8. DSC curves of L50 (-) and the composite with L50 at $\phi_f = 1.0$ (- -).

and differential of heat capacity at T_g (ΔC_p) of the PMMA-*block*-P(MMA-*co*-HEMA) block-random copolymers and the composites was determined by DSC. For diblock copolymer, two values of T_g are generally expected when each block sequence is incompatible. However, the single T_g value was observed at 119.7°C for L50. The ΔC_p of L50 was 0.231 J/gK. The T_g values of PMMA and PHEMA are 108 and 118°C, respectively. Here it should be noticed that the L50 was block-random copolymer. Moreover, the MMA was a common unit for the block and the random sequences. The single T_g indicates that the microphase separation was not formed for L50. It would be due to the low segregation of HEMA units in the P(MMA-*co*-HEMA) sequence. This agreed with the fact that the microphase separation of L50 was not observed by TEM. Similar results were observed for L25 and R50. Thus, it was thermo-analytically confirmed that microphase separation did not occur for PMMA-*block*-P(MMA-*co*-HEMA) block-random copolymer films. For the DSC curves of the composites, T_g peak was not observed. It would be due to the fact that the mobility of the organic chain was hindered by silica-rich domains.

In order to investigate the hybridization effects on thermal stability of the composites, TGA and DTG curves of L50 and the composites were measured and are shown in Figs. 9 and 10, respectively. For L50, as a typical precursor organic copolymer, three-step decrease of weight was observed. The first decrease of weight (near 100°C) was related to the evaporation of casting solvents and water. According to Kashiwagi et al., the second (T_2, 293.6°C) and third (T_3, 383.7°C) peaks in the DTG curve indicate the degradation of vinylidene chain end and random initiation by unzipping of methacrylate chain, respectively.[26] For the composites, three-step decrease of weight was also observed as well as L50. T_2 and T_3 were listed in Table 4. The degradation owing to the head to head linkage (around 195°C) was not observed for L50. L50 was completely degradated at 440°C. In contrast to L50, the composites was not completely degradated at 500°C. By

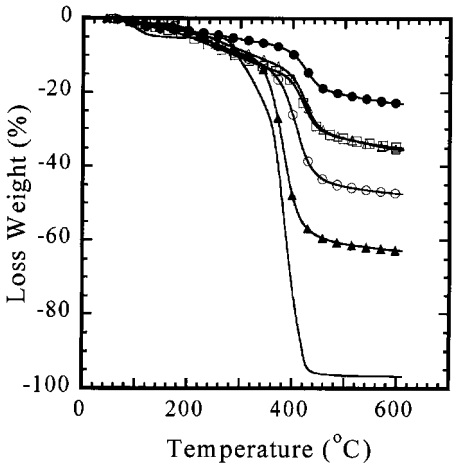

Figure 9. TGA curves of the organic copolymer and the composites. (-): L50, (▲): the composite with L25 at $\phi_f = 0.5$, (○): the composite with L25 at $\phi_f = 1.0$, (□): the composite with L50 at $\phi_f = 1.0$, (△): the composite with R50 at $\phi_f = 0.5$, (●): the composite with R50 at $\phi_f = 1.0$.

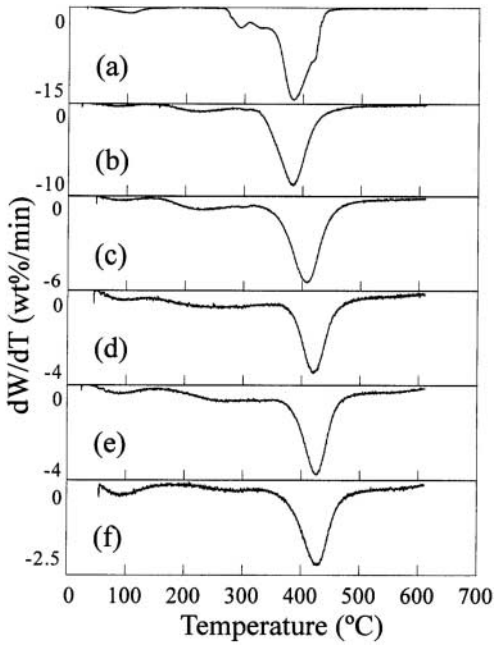

Figure 10. DTG curves of the organic copolymer and the composites. (a) L50, (b) the composite with L25 at $\phi_f = 0.5$, (c) the composite with L25 at $\phi_f = 1.0$, (d) the composite with L50 at $\phi_f = 1.0$, (e) the composite with R50 at $\phi_f = 0.5$, (f) the composite with R50 at $\phi_f = 1.0$.

Table 4. Thermal properties of L50 and the composites.

Code	ϕ_f[a]	Weight fraction of silica[b]	Y_c[c]	Peak temperature[d] (°C)	
				Second	Third
L50	0	0	0.032	293.6	383.7
L25-0.5	0.5	0.318	0.374	223.9	383.9
L25-1.0	1.0	0.483	0.527	224.4	409.2
L50-1.0	1.0	0.668	0.652	257.4	421.2
R50-0.5	0.5	0.582	0.647	269.0	426.5
R50-1.0	1.0	0.735	0.771	293.5	426.3

[a] The molar ratio of PHPS to hydroxyl groups in feed.
[b] Weight fraction of silica in the composite calculated from the ϕ_f values.
[c] Char residue at 600°C determined by TGA curves.
[d] Determined by DTG curves.

increase of the weight fraction of the silica in the composites, T_2 of the composite decreased to 223.9°C at first, and then started to increase up to 293.5°C. T_3 value was simply increased to 426°C with the weight fraction of the silica. The char residue (Y_c) at 600°C and weight fraction of silica of the composites are listed in Table 4. As well as previous study,[17] the Y_c values and the weight fractions of silica were well agreed. It was concluded that organic component in the composite did not exist at 600°C. Consequently, it was found that the thermostability of the composites was increased by hybridization.

CONCLUSION

In order to investigate the effects of the distribution of HEMA units in the organic copolymer on the reaction of PHPS with the organic copolymer and the microphase separation of nano-composites, three types of PMMA-*block*-P(MMA-*co*-HEMA) block-random copolymer were synthesized as precursors of the PMMA/silica-rich nano-composites. For the reaction of PHPS with PMMA-*block*-P(MMA-*co*-HEMA) block-random copolymers, the increasing tendency of ϕ_p with ϕ_f was independent on the distribution of HEMA units in PMMA-*block*-P(MMA-*co*-HEMA) block-random copolymers when the molar fraction of HEMA in P(MMA-*co*-HEMA) block was in a range from 0.25 to 0.5. The calcination of PHPS to silica in the composites was completed after casting without heating. All composite films were transparent except for the composites with R50 at $\phi_f = 1.0$ and 1.5. From TEM observation of the composites with L25, the small silica-rich domain (< 10 nm) was observed. For the composites with L50 and R50, the spherical organic domains with the diameters of ca. 30 nm were observed. The sub-micrometer silica-rich domains were also observed for the composites with R50 at $\phi_f = 1.0$ and 1.5. To control of the morphology of the nano-composites, it was important to change the composition of block copolymer rather than the amount of PHPS in feed. From the SEM observation, it was found that the silica-rich domains were homogeneously dispersed in the wide area of the nano-composites. The thermal stability of the composite was increased with the weight fraction of silica. The peak temperature of the third degradation of organic compound, T_3, was saturated at 426°C.

ACKNOWLEDGMENT

The authors are greatful to the financial support by "Tokuyama Science Foundation."

REFERENCES

1. Alexandre, M.; Dubois, P. Polymer-layered silicate nanocomposites: preparation, properties and use of a new class of materials. Mater. Sci. Eng. **2000**, *28* (1–2), 1–63.
2. Werne, von T.; Patten, T.E. Preparation of structurally well-defined polymer-nanoparticle hybrids with controlled/living radical polymerizations. J. Am. Chem. Soc. **1999**, *121* (32), 7409–7410.

3. Senkevich, J.J.; Desu, S.B. Near-room-temperature thermal chemical vapor deposition of poly(chloro-*p*-xylylene)/SiO_2 nanocomposites. Chem. Mater. **1999**, *11* (7), 1814–1821.
4. Zheng, L.; Farris, R.J.; Coughlin, E.B. Novel polyolefin nanocomposites: synthesis and characterizations of metallocene-catalyzed polyolefin polyhedral oligomeric silsesquioxane copolymers. Macromolecules **2001**, *32* (23), 8034–8039.
5. Suh, D.J.; Lim, Y.T.; Park, O.O. The property and formation mechanism of unsaturated polyester-layered silicate nanocomposite depending on the fabrication methods. Polymer **2000**, *41* (24), 8557–8563.
6. Wen, J.; Wilkes, G.L. Organic/inorganic hybrid network materials by the sol–gel approaches. Chem. Mater. **1996**, *8* (8), 1667–1681.
7. Saegusa, T.; Chujo, Y. Organic/inorganic hybrid polymer. J. Macromol. Sci. Chem. **1990**, *A27* (13–14), 1603–1612.
8. Mark, J.E. Ceramic-reinforced polymers and polymer modified ceramics. Polym. Eng. Sci. **1996**, *36* (24), 2905–2920.
9. Gao, Z.; Zhao, Z.; Ou, Y.; Qi, Z.; Wang, F. Preparation of styrene-maleic anhydride copolymer/Si—O network nanocomposites by the sol–gel process. Polym. Int. **1996**, *40* (3), 187–192.
10. Melosh, N.A.; Lipic, P.; Bates, F.S.; Wudl, F.; Stucky, G.D.; Fredrickson, G.H.; Chmelka, B.F. Molecular and mesoscopic structures of transparent block copolymer-silica monoliths. Macromolecules **1999**, *32* (13), 4332–4342.
11. Tian, D.; Dubios, Ph.; Jérôme, R. Biodegradable and biocompatible inorganic–organic hybrid materials I. Synthesis and characterization. J. Polym. Sci. A: Polym. Chem. **1997**, *35* (11), 2295–2309.
12. Rajan, G.S.; Mark, J.E.; Seabolt, E.E.; Ford, W.T. Thermal and mechanical properties of some poly(methly methacrylate)/silica composites with intentionally suppressed interfacial bonding. J. Macromol. Sci.-Pure Appl. Chem. **2002**, *A39* (1–2), 39–51.
13. Severdia, A.G.; Low, M.J.D. An infrared study of the reactions of mono- and trimethylamine with Si—O—$SiHCl_2$ monolayers on silica. Langmuir **1988**, *4* (6), 1234–1239.
14. Low, M.J.D.; Severdia, A.G.; Chan, J. Infrared study of the sorption of $HSiCl_3$ on silica and the stability of the chemisorbed layers. J. Colloid Interf. Sci. **1982**, *86* (1), 111–118.
15. Saito, R.; Kuwano, K.; Tobe, T. Synthesis of poly(methyl methacrylate)-silica nano-composite. J. Macromol. Sci.-Pure Appl. Chem. **2002**, *A39* (3), 171–182.
16. Molau, G.E. *Block Copolymers*; Plenum Press: New York, 1970.
17. Saito, R.; Mori, Y. Synthesis of poly(methyl methacrylate)-silica nano-composites 2: poly[methyl methacrylate-*block*-(methyl methacrylate-*co*-2-hydroxyethyl methacrylate)]. J. Macromol. Sci.-Pure Appl. Chem. **2002**, *A39* (9), 915–934.
18. Matyjaszewski, K.; Xia, J. Atom transfer radical polymerization. Chem. Rev. **2001**, *101* (9), 2921–2990.
19. Shipp, D.A.; Wang, J.L.; Matyjaszewski, K. Synthesis of acrylate and methacrylate block copolymers using atom transfer radical polymerization. Macromolecules **1998**, *31* (23), 8005–8008.

20. Beers, K.L.; Boo, S.; Gaynor, S.G.; Matyjaszewski, K. Atom transfer radical polymerization of 2-hydroxyethyl methacrylate. Macromolecules **1999**, *32* (18), 5772–5776.
21. Zhang, X.; Xia, J.; Matyjaszewski, K. Controlled/living radical polymerization of 2-(dimethylamino)ethyl methacrylate. Macromolecules **1998**, *31* (15), 5167–5169.
22. Gall, W.G.; McCrum, N.G. Internal friction in stereoregular polymethyl methacrylate. J. Polym. Sci. **1961**, *50* (154), 489–495.
23. Shen, M.C.; Strong, J.D.; Matusik, F.J. The effect of hydrogen bonds on the dynamic mechanical properties of glassy polymethacrylates from 77°K. J. Macromol. Sci. (Phys.) **1967**, *B1* (1), 15–27.
24. Okano, T.; Aoyagi, J.; Shinohara, I. The wettability and composition of 2-hydroxyethyl methacrylate copolymers. Nippon Kagakukaishi **1976**, (1), 161–165.
25. Shimizu, Y.; Yamada, K.; Aoki, T.; Tashiro, Y.; Funayama, T. Method for forming high purity siliceous film and high purity siliceous film. JP Patent 11-105187 Apr. 20, 1999.
26. Kashiwagi, T.; Inaba, A.; Brown, J.E.; Hatada, K.; Kitayama, T.; Masuda, E. Effects of weak linkages on the thermal and oxidative degradation of poly(methyl methacrylates). Macromolecules **1986**, *19* (8), 2160–2168.

Received October 2002
Revision received February 2003